Walisongo Journal of Chemistry
Walisongo Journal of Chemistry Vol. 9 Issue 1 (2026), 15-27
ISSN: 2621-5985 (online); 2549-385X (print)
DOI: https://doi.org/10.21580/wjc.v9i1.28939

PURIFICATION OF CRUDE GLYCEROL USING KOH-ACTIVATED CORNCOB CARBON AND ITS UTILIZATION AS A MOISTURIZING AGENT IN LIQUID SOAP

Amalia Qurrata A'yun, Adilah Aliyatulmuna*, Rosanina Kartika Santana, Felda Mufarrihati

Department of Chemistry, Faculty of Mathematics and Natural Sciences, Universitas Negeri Malang

*Corresponding author: adilah.aliyatulmuna.fmipa@um.ac.id

Abstract

The purification of crude glycerol was carried out through an antisolvent treatment process followed by adsorption. The antisolvent treatment was performed using methanol, while adsorption was conducted using corncob biomass waste. Corncob carbon was activated with 20% KOH, followed by calcination at 400°C for 2 hours. The IR spectrum of the activated carbon showed the presence of -C=C and -C-H functional groups. The diffraction pattern of the activated carbon, with peaks at 2θ ≈ 23.3° and 41.3°, indicated an amorphous structure and an imperfect crystalline graphite structure. The antisolvent treatment process involved the addition of methanol to crude glycerol at a ratio of 3:1, followed by vacuum filtration and evaporation. The adsorption process was carried out using 0.5 g of activated carbon for 75 minutes, producing glycerol with a glycerol content of 96.29%, water content of 3.21%, ash content of 6.05%, and free fatty acid content of 0.21%. These results were in accordance with SNI 06-1564-1989 concerning crude glycerol and SNI 06-2570-1992 concerning technical glycerol. The IR spectrum of glycerol showed characteristic peaks corresponding to -O-H and -C-H groups. The obtained glycerol was used as a moisturizing agent in liquid soap. The resulting liquid soap had a pH range of 5.20-5.67 and an FFA content range of 0.57-0.60, which complied with SNI 2588:2017 concerning liquid hand soap.

Keywords: *Crude Glycerol, Corncobs, Antisolvent Treatment, Adsorption, Liquid Soap*

Introduction

Crude glycerol is the main by-product of biodiesel production, comprising approximately 10% of each batch. It contains 77–90% glycerol, along with impurities such as water, methanol, fatty acids, esters, and salts, including NaCl or K_2SO_4 (1). These impurities limit its direct application; therefore, purification is required before crude glycerol can be used in the food, cosmetic, and pharmaceutical industries. Common purification methods include vacuum distillation, ion exchange, and activated carbon adsorption. Among these methods, activated carbon adsorption is considered the most efficient and cost-effective (2).

An ideal adsorbent should be eco-friendly, cost-effective, non-toxic, stable, and have a high adsorption capacity. Indonesia, as an agricultural country, generates large amounts of agricultural waste, including corncobs. In 2024, corn production reached approximately 15.21

million tons, with corncobs accounting for roughly 3 million tons (3). Corncobs contain high amounts of cellulose (41%), hemicellulose (36%), and lignin (16%), making them suitable adsorbents for removing metals, dyes, and other substances (4).

A previous study revealed that corncob powder with a particle size of 100 mesh can effectively reduce the turbidity of used cooking oil because of its high adsorption capacity (4). However, crude glycerol contains different types of impurities, such as inorganic salts, free fatty acids (FFAs), and colorants. Therefore, the effectiveness of corncob-based carbon, particularly in its non-activated form, remains uncertain.

Corncobs can be transformed into activated carbon through two main steps: carbonization and activation. Carbonization decomposes organic components, mainly cellulose, into elemental carbon, while activation through chemical, physical, or physicochemical methods enhances the surface area of the carbon (5). In this study, chemical activation using potassium hydroxide (KOH) was employed because of its strong basicity, hygroscopic nature, and effectiveness in removing impurities, resulting in activated carbon with a high surface area. KOH-activated carbon is known to be highly microporous and more efficient than carbon activated using $ZnCl_2$ or H_3PO_4. Following activation, the material was calcined at 400°C to eliminate volatile compounds and residual tar, thereby further improving its adsorption properties (6).

Adsorption using KOH-activated carbon is more effective when applied as a final step after initial separation processes. One such preliminary method is antisolvent treatment, which enhances glycerol purity by precipitating salt impurities. Antisolvents such as ethanol, methanol, and propanol are commonly used for this purpose. The process involves adding an antisolvent to crude glycerol, followed by vacuum filtration and evaporation, effectively reducing impurities before the adsorption stage (7).

This research aims to increase glycerol purity through adsorption using carbon derived from corncobs pre-activated with 20% KOH. The study seeks to obtain glycerol with higher purity, which can subsequently be used as a humectant in liquid soap.

Experimental Section

Materials

The materials used included crude glycerol from PT Graha Jaya Pratama Kinerja; corncobs from Grobogan Regency, Central Java; distilled water; solid NaOH (Merck); solid KOH (Smart Lab); $NaIO_4$; 0.2 N H_2SO_4 solution; 0.1 N iodine solution; 1% phenolphthalein indicator; bromothymol blue indicator; 1% starch indicator; 1 N HCl solution; methanol; ethylene glycol; 96% ethanol; 0.1 N $Na_2S_2O_3$ solution; SLES solution (sodium lauryl ether sulfate); solid NaCl; solid sodium sulfate; 0.1% EDTA solution; amphitol solution; strawberry fragrance; and methylene blue.

Instruments

The instruments used included an analytical balance (Shimadzu ATX 224), oven (Memmert), furnace (B-One), hot plate with magnetic stirrer, water bath shaker, rotary evaporator (IKA® RV 10), Buchner vacuum filtration setup (IKA® MVP 10 basic), pH meter, SEM-EDX instrument (Zeiss Bruker), FTIR spectrometer (Shimadzu IRPrestige-21), BET surface area analyzer (Micromeritics Tristar II), surface tension meter (YJINGRUI BZY-102), and gas chromatography-mass spectrometry instrument (GC-MS, Agilent 5977B).

Procedure

This study involved the preparation of activated carbon from corncobs, purification of crude glycerol, and formulation of liquid soap using the purified glycerol. Corncobs were carbonized at 450°C and chemically activated with 20% KOH, followed by calcination at 400°C. The resulting activated carbon was

characterized using FTIR, SEM-EDX, XRD, and BET analysis. Crude glycerol was purified through antisolvent treatment using methanol, vacuum filtration, evaporation, and adsorption with activated carbon, with variations in adsorbent mass and contact time. The purified glycerol was analyzed for water content, ash content, glycerol concentration, and free fatty acid content. Finally, liquid soap was formulated using different concentrations of purified glycerol and evaluated for pH, free fatty acid content, moisture retention, emulsion type, and surface tension to ensure compliance with hand soap quality standards.

Preparation of Activated Carbon

Corncobs were first washed, cut into smaller pieces, and dried in an oven at 70°C for 24 hours. The dried material was then carbonized at 450°C for 10 minutes to produce raw carbon. The carbon was activated by mixing 2 g of carbon powder, sieved to 100 mesh, with 20 mL of 20% KOH solution and stirring at 700 rpm for 4 hours. The mixture was filtered and oven-dried at 110°C for 120 minutes, followed by calcination in a furnace at 400°C for 2 hours (8). The resulting carbon was neutralized using a 1 N HCl solution and dried again. The carbon was then analyzed based on several parameters according to SNI 06-3730-1995 and characterized using FTIR (Fourier-transform infrared), SEM-EDX, XRD, and BET surface area analysis.

Purification of Crude Glycerol

This process involved several steps. Initially, methanol was added as an antisolvent at a glycerol-to-solvent volume ratio of 1:3 to precipitate inorganic salts. The mixture was vacuum-filtered to separate the precipitates and then evaporated at 70°C for 2 hours to remove methanol and reduce the water content. Subsequently, the semi-purified glycerol underwent adsorption using 0.5 g of activated carbon for 75 minutes. The adsorption process was conducted in a water bath shaker at 200 rpm (2). The purified glycerol was then analyzed for water content, ash content, glycerol content, and FFA levels according to SNI 06-1564-1989 and SNI 06-2570-1992. In addition, FTIR and GC-MS characterization were performed to analyze the glycerol.

Soap Production

The final stage of the study was the production of liquid soap using the purified glycerol. A base formula was prepared by mixing 12% sodium lauryl ether sulfate (SLES), 5% NaCl, 4% sodium sulfate, and 0.1% EDTA. Then, 1% amphitol and varying concentrations of glycerol, namely 0%, 0.8%, 1%, 1.2%, 1.4%, and 1.6%, were added, resulting in six different formulations, including a control sample. One additional soap formulation was prepared using glycerol purified with non-activated carbon. Each formulation was diluted with distilled water to a total volume of 100 mL and left to stand for 24 hours (9). The resulting soap samples were evaluated in accordance with SNI 2588-2017 for liquid hand soap. The tests included pH measurement using a pH meter, FFA determination by titration with KOH, and moisture analysis using a skin analyzer before and after soap application. The emulsion type was identified by adding methylene blue to the soap and observing color dispersion to determine whether the emulsion was oil-in-water or water-in-oil. Surface tension was also measured using a surface tension meter. These tests were performed to assess the quality and functionality of the liquid soap formulated with glycerol derived from corncob-based activated carbon.

Results and Discussion

Carbonization and Activation of Carbon

Corncobs were carbonized through thermal decomposition under limited oxygen conditions to remove non-carbon elements and produce a porous carbon structure. The process involved four stages: initial dehydration at 25–150°C, glycosidic bond cleavage and cyclic structure formation at 150–240°C, thermal

breakdown and volatile release at 240–400°C, and final aromatization, which formed layered carbon structures. This method effectively converted cellulose into fixed carbon, forming a rudimentary porous matrix suitable for further activation (10).

Figure 1. Activated carbon

Chemical activation followed by physical treatment was employed to enhance the adsorptive properties of the carbon. The carbon was soaked in 20% KOH solution, which promoted the development of microporous structures and increased surface functionality. This was followed by calcination at 400°C for 2 hours, which enhanced pore formation through gas-phase reactions and facilitated the release of potassium ions during washing (11). These steps significantly improved the structural and adsorptive qualities of the carbon, making it suitable for glycerol purification (12). The activated carbon is shown in **Figure 1**.

Table 1. Comparison of iodine adsorption capacity, moisture content, and ash content

Parameter	Unactivated carbon	5% KOH-activated carbon	20% KOH-activated carbon	SNI 06-3730-1995
Iodine adsorption capacity (mg/g)	734.20	918.78	985.72	>750
Moisture content (%)	13.04	6.06	2.23	<15
Ash content (%)	2.96	-	5.54	<10

Analysis of Activated Carbon Based on SNI 06-3730-1995

The characterization parameters of activated carbon included iodine adsorption capacity, moisture content, and ash content. The iodine adsorption value was determined using iodometric titration, and the results indicated that activated carbon had a larger surface area than unactivated carbon (13). The decrease in moisture content with increasing KOH concentration confirms the role of KOH as a dehydrating agent, resulting in lower hygroscopicity in the activated carbon (14). Based on iodine adsorption capacity and moisture content, carbon activated with 20% KOH was selected as the optimal adsorbent. Furthermore, the ash content of the 20% KOH-activated carbon increased from 2.96% to 5.54%, which can be attributed to the reaction of KOH with inorganic components during activation and subsequent heating at 400°C, producing mineral residues (15).

Characterization of Activated Carbon

Surface Morphology and Identification of Activated Carbon Elements

Scanning electron microscopy (SEM) was used to observe the surface morphology of the corncob-derived carbon before and after activation. **Figure 2** shows that the unactivated carbon had a relatively compact structure with few and poorly developed pores, primarily due to residual impurities that blocked pore formation. In contrast, carbon activated with 20% KOH exhibited a well-developed porous structure with more visible and larger pores. The improved porosity can be attributed to the

depolymerization and volatilization of organic compounds during carbonization and activation, which effectively ruptured the pore walls and facilitated the creation of new pores (16). This structural transformation enhanced the adsorptive surface area of the activated carbon, making it more effective for adsorption applications.

Table 2. Elemental composition of unactivated carbon and 20% KOH-activated carbon

Material	Element Content (%wt)		
	C	O	K
Unactivated carbon	78.90	19.82	0.53
20% KOH-activated carbon	82.31	16.96	0.29

Energy-dispersive X-ray spectroscopy (EDX) analysis provided elemental composition data that supported the morphological findings. As shown in **Table 2**, the carbon content increased from 78.90% in unactivated carbon to 82.31% in activated carbon, while the oxygen content decreased from 19.82% to 16.96%. This shift indicates the removal of oxygen-containing functional groups and moisture during the activation and calcination processes (17). In addition, the potassium (K) content decreased after activation due to its removal during the acid-washing stage, demonstrating the successful removal of excess activating agent (18).

Identification of Activated Carbon Functional Groups

FTIR spectroscopy was used to identify the functional groups present on the surface of the carbon samples. The FTIR spectra of 20% KOH-activated carbon and unactivated carbon are shown in **Figure 3**. In the unactivated carbon, several characteristic absorption bands were observed: a broad O-H stretching vibration at approximately 3365 cm^{-1}, indicating the presence of hydroxyl groups or adsorbed water; C-H stretching at approximately 2916 and 2852 cm^{-1}, associated with aliphatic -CH, $-CH_2$, and $-CH_3$ groups; and C=O and C=C stretching at approximately 1683 and 1575 cm^{-1}, respectively, indicating the presence of carbonyl and aromatic structures. These functional groups originated from the partial decomposition of lignocellulosic biomass and incomplete carbonization (19).

In contrast, as shown in **Figure 3**, the FTIR spectrum of the KOH-activated carbon revealed significant changes. The O-H and aliphatic C-H bands were largely absent, suggesting effective dehydroxylation and decarboxylation during activation and calcination. The aromatic C=C peak shifted slightly to a lower wavenumber, approximately 1565 cm^{-1}, indicating an increase in conjugated carbon structures. The absence of C-O and C=O bands in the activated carbon also reflected the breakdown of oxygenated groups and the enhancement of the carbon network. These spectral changes confirm that KOH activation and thermal treatment effectively modified the chemical surface of the carbon, reduced polarity, and improved its suitability for hydrophobic or organic pollutant adsorption (20).

Carbon Diffraction Pattern

The XRD diffraction patterns of both unactivated and KOH-activated carbon are shown in **Figure 4**. Both samples exhibited broad diffraction peaks in the 2θ range of 20°–30°, which are characteristic of amorphous carbon with a turbostratic structure. The unactivated carbon showed a major peak at $2\theta \approx 24.9°$, corresponding to the (002) plane of disordered graphite-like carbon (21). After activation, the XRD pattern showed a slightly sharper peak at $2\theta \approx 23.3°$, indicating a more ordered but still predominantly amorphous structure. In addition, a small peak at $2\theta \approx 41.3°$, attributed to the (100) plane, confirmed the partial development of graphitic domains. These results suggest that although the carbon remained largely amorphous, KOH activation slightly enhanced its microstructural ordering (22).

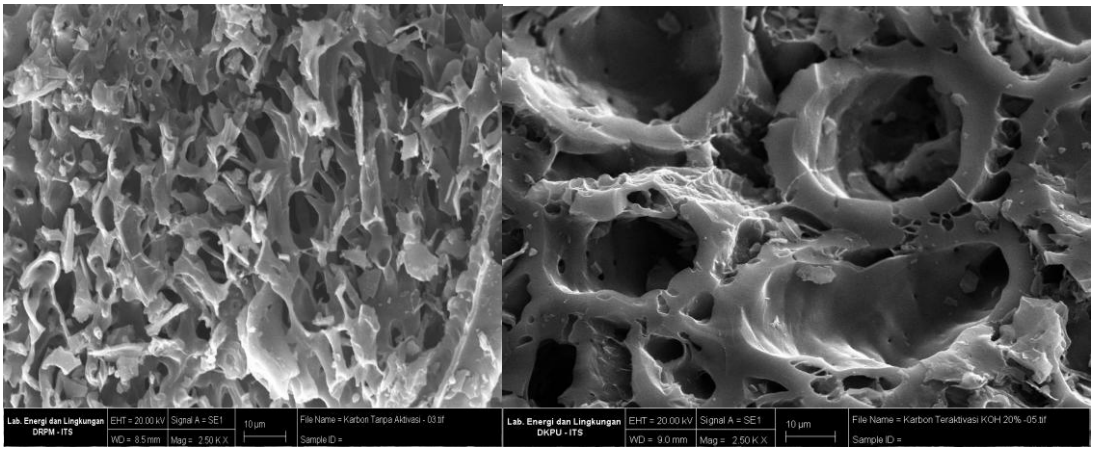

(a) *(b)*

Figure 2. Morphology of unactivated carbon (a) and 20% KOH-activated carbon (b) (magnification: 250 KX; scale bar = 10 µm)

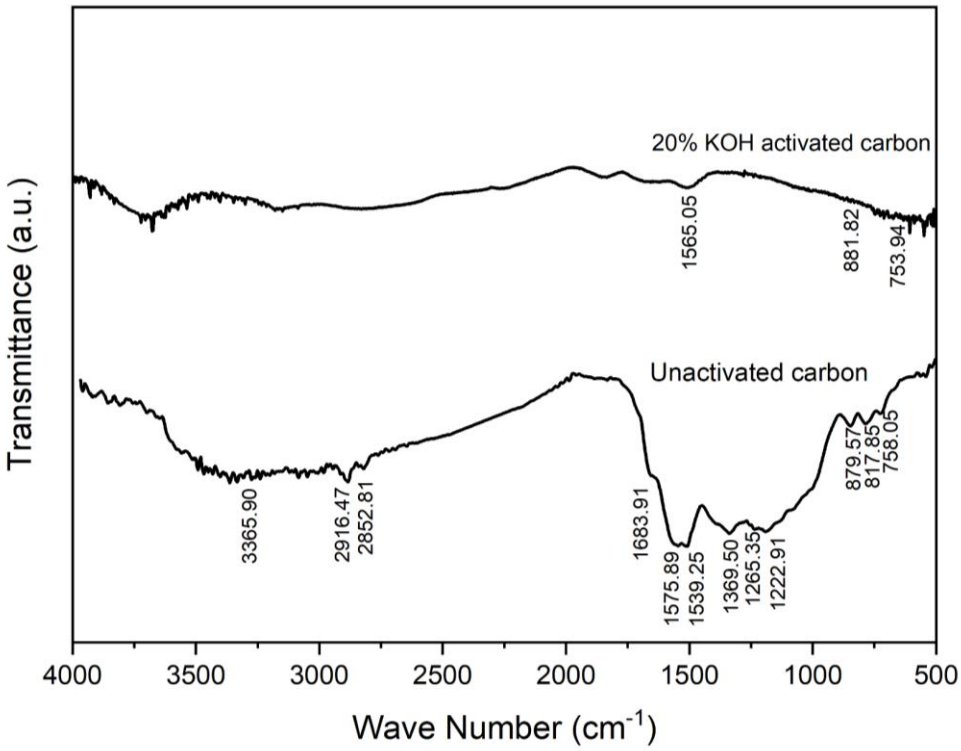

Figure 3. FTIR spectra of 20% KOH-activated carbon and unactivated carbon

Brunauer-Emmett-Teller (BET) surface area analysis revealed a substantial increase in surface area after activation. As shown in **Table 3**, unactivated carbon exhibited a relatively low surface area of 11.16 m^2/g, whereas KOH-activated carbon showed a dramatic increase to 356.29 m^2/g. This enhancement can be attributed to the chemical etching action of KOH, which generated a high density of micropores and mesopores by removing carbon atoms and promoting pore development. The subsequent calcination step at 400°C further stabilized the porous structure and eliminated volatile residues. The increased surface area significantly improved the adsorptive capacity of the activated carbon, making it highly effective for applications

Copyright © 2026 WJC | ISSN 2621-5985 (online) | ISSN 2549-385X (print)
Volume 9, Nomor 1, 2026

such as glycerol purification and other liquid-phase adsorption processes (23).

Surface Area of Activated Carbon

Table 3. Surface area of unactivated carbon and 20% KOH-activated carbon

Corncob carbon type	Surface area (m^2/g)
Unactivated carbon	11.16
20% KOH-activated carbon	356.29

Glycerol Concentration Enhancement

Glycerol purification was achieved through two main steps: antisolvent treatment and adsorption. Methanol was added to crude glycerol at a ratio of 3:1, selectively precipitating inorganic salts while maintaining glycerol solubility (24). The precipitated salts are shown in **Figure 5**.

Figure 5. Precipitated salts

The mixture was then vacuum-filtered and evaporated at 70°C to remove excess methanol and water. The resulting semi-purified glycerol underwent further purification through adsorption using KOH-activated carbon. This process effectively removed residual impurities, such as water, salts, and free fatty acids, significantly increasing glycerol purity to 96.29%. This improvement was indicated by analytical results and visual changes, as the sample changed from brownish to clear yellow, as shown in **Figure 6**. The increase in glycerol content is presented in **Table 4**.

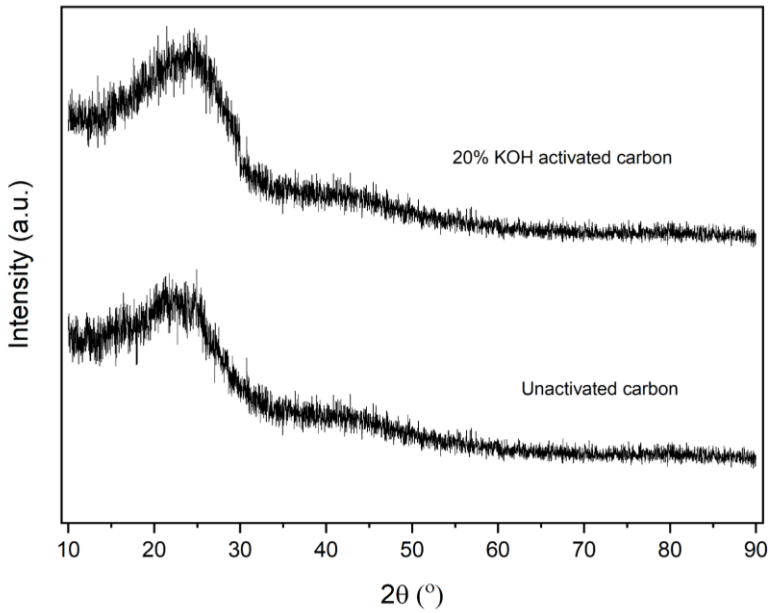

Figure 4. XRD diffraction patterns of 20% KOH-activated carbon and unactivated carbon

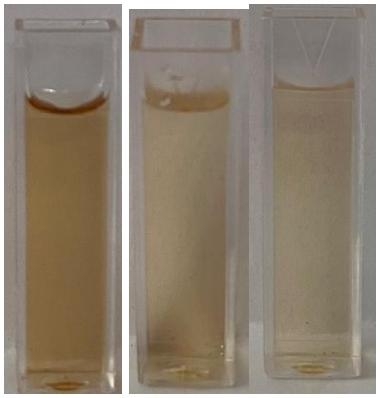

(a) (b) (c)

Figure 6. (a) Crude glycerol, (b) crude glycerol after methanol addition and evaporation, and (c) glycerol obtained after adsorption

Table 4. Increase in glycerol content

Composition	Crude glycerol	After antisolvent treatment	After adsorption	SNI 06-1564-1989 crude glycerol	SNI 06-2570-1992 technical glycerol
Glycerol (%)	61.87	83.06	96.29	> 80	> 87
Water (%)	28.31	9.96	3.24	< 10	-
Ash (%)	7.36	6.51	6.05	< 10	-
FFA (%)	0.62	0.55	0.21	-	<0.025
Liquid appearance	Thick, cloudy, yellowish brown	Thick, clear, yellow	Thick, clear, yellow	-	Thick, clear, colorless to yellowish
Density (g/mL)	1.109	1.251	1.295	-	>1.228

Characterization of Glycerol

Identification of Glycerol Functional Groups

FTIR analysis was conducted to identify changes in functional groups between crude and purified glycerol. As shown in **Figure 7**, both spectra showed characteristic O-H and C-H absorption bands; however, noticeable shifts indicated successful purification. The broad O-H stretching peak in crude glycerol at 3300.01 cm^{-1} shifted to 3293.56 cm^{-1} in purified glycerol, suggesting stronger hydrogen bonding due to impurity removal. C-H stretching and bending vibrations were observed in the 2940–2860 cm^{-1} and 1457–1411 cm^{-1} regions, while primary alcohol C-O stretching appeared at approximately 1210 and 1108 cm^{-1} in both samples. A peak near 1653 cm^{-1} in crude glycerol, associated with ester groups, shifted in the purified sample, indicating a decrease in ester content (25).

GC-MS Analysis of Glycerol

The results of glycerol purification showed a significant improvement in glycerol content after antisolvent treatment followed by adsorption using corncob-based activated carbon. As shown in **Figure 8**, gas chromatography-mass spectrometry (GC-MS) analysis revealed that the major component of the purified sample was glycerol, also known as 1,2,3-propanetriol, with a relative peak area of 99.51% at a retention time of 9.646 minutes. This high percentage confirms the effectiveness of the purification steps in removing impurities such as fatty acid methyl esters, which were detected only in trace amounts of less than 0.3% (26).

The minor peaks identified in the chromatogram corresponded to methyl esters, such as methyl palmitate and methyl oleate, indicating residual but minimal contamination from fatty acid derivatives. The dominance of glycerol in the sample confirmed the successful separation of non-glycerol compounds and the substantial increase in purity.

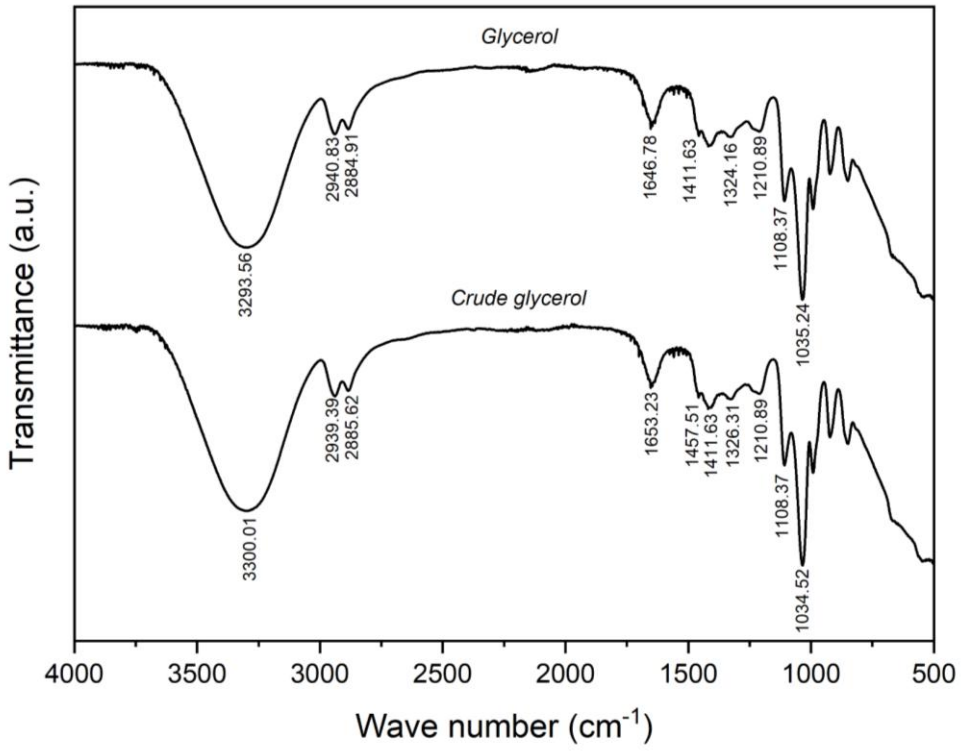

Figure 7. FTIR spectra of crude glycerol and purified glycerol

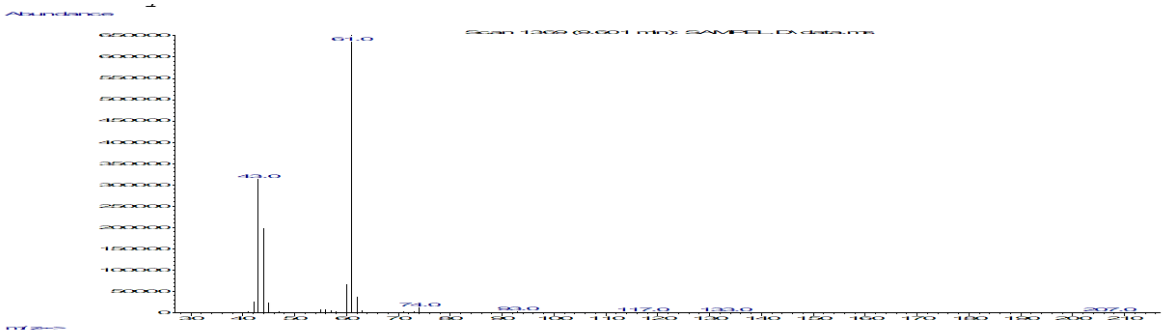

Figure 8. Chromatogram of purified glycerol

Soap Production

The liquid soap formulation process was carried out by varying the concentration of glycerol as a humectant. The effect of glycerol addition on the soap was then analyzed according to the test parameters specified in SNI 2588-2017 for liquid hand soap. The analysis results are presented in **Table 5**. The produced soap is shown in **Figure 9**.

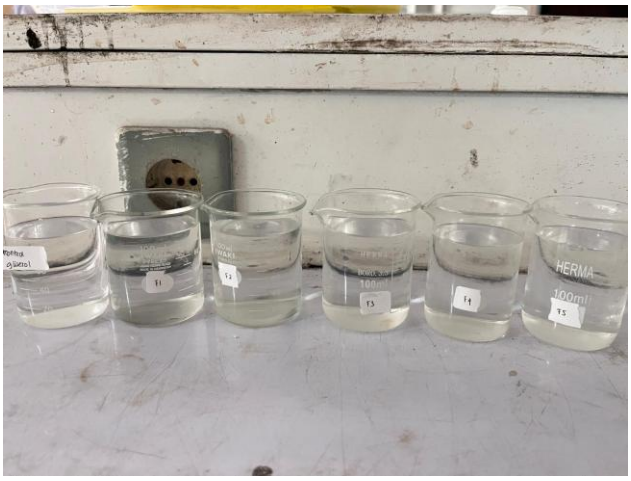

Figure caption:
K : Control
F1 : 0.8% glycerol
F2 : 1% glycerol
F3 : 1.2% glycerol
F4 : 1.4% glycerol
F5 : 1.6% glycerol

Figure 9. Soap produced with various concentrations of glycerol

Table 5. Analysis results of glycerol addition

Parameter	K	TA	F1	F2	F3	F4	F5	SNI 2588-2017 liquid hand soap
Glycerol (%)	0	0.8	0.8	1	1.2	1.4	1.6	-
Moisture (%)	32	35	44	Max = 60	Max = 60	Max = 60	Max = 60	-
Surface tension (mN/m)	148.9	144.3	126.4	94.5	90.3	86.4	85.5	-
pH	5.60	5.67	5.29	5.20	5.50	5.64	5.33	4-10
FFA (%)	0.57	1.23	0.59	0.60	0.59	0.60	0.59	<1
Emulsion type	Oil-in-water							

Notes: K : control; TA : 0.8% glycerol purified with non-activated carbon; F1 : 0.8% glycerol; F2 : 1% glycerol; F3 : 1.2% glycerol; F4 : 1.4% glycerol; F5 :1.6% glycerol

Glycerol in liquid soap formulations increased skin moisture content. As shown in **Table 5**, glycerol concentrations of 0%, 0.8%, and ≥1% resulted in moisture levels of 32%, 44%, and a maximum value of 60%, respectively. The formulation containing 0.8% glycerol purified with non-activated carbon (TA) yielded lower skin moisture than the formulation containing the same concentration of glycerol purified with KOH-activated carbon (F1).

The surface tension of the soap decreased when the glycerol concentration exceeded 0.8%. This suggests that glycerol at concentrations above 0.8% contributes to surface-active behavior in the soap solution. Compounds synthesized from glycerol have been shown to exhibit surfactant properties (27).

Based on Table 5, the pH and FFA values of the liquid soap met the requirements of SNI 2588-2017 for liquid hand soap. Variations in glycerol concentration from 0% to 1.6% did not significantly affect the pH or FFA values of the soap. This result is consistent with the study by Aras and Lestari (9), who also investigated variations in glycerol concentration in soap formulations.

In this study, an emulsion test was also performed on the liquid soap. The emulsion test involved adding a methylene blue solution to the soap sample and homogenizing the mixture. The resulting homogeneous mixture indicated that the soap emulsion type was oil-in-water.

Conclusion

Corncob-derived activated carbon treated with 20% KOH can be effectively used as an adsorbent to enhance glycerol purity. The activated carbon exhibited a porous structure, with carbon (C), oxygen (O), and potassium (K) as the predominant elements. Functional groups such as C=C and C-H were identified on its surface. X-ray diffraction analysis revealed an amorphous structure with partially developed graphitic crystallinity. Following activation, the surface area increased to 356.29 m^2/g. Glycerol purification through antisolvent treatment and adsorption yielded a purity of 96.29%, achieved using 0.50 g of adsorbent and an adsorption time of 75 minutes. The purified glycerol was subsequently used as a moisturizing agent in a liquid soap formulation. The resulting liquid soap complied with the Indonesian National Standard, SNI 2588-2017, for liquid hand soap based on pH and FFA parameters.

Acknowledgement

The authors express their sincere gratitude to Universitas Negeri Malang for the financial assistance provided under Contract Number 24.2.630/UN32.14/LT/2025.

References

[1] S. M. Ioannidou *et al.*, "Sustainable Production of Bio-Based Chemicals and Polymers via Integrated Biomass Refining and Bioprocessing in A Circular Bioeconomy Context," *Bioresour. Technol.*, vol. 307, Art. no. 123093, pp. 1–14, 2020, doi: 10.1016/j.biortech.2020.123093

[2] T. Attarbachi, M. Kingsley, and V. Spallina, "Experimental Scale-Up and Technoeconomic Assessment of Low-Grade Glycerol Purification from Waste-Based Biorefinery," *Ind. Eng. Chem. Res.*, vol. 63, no. 11, pp. 4905–4917, 2024, doi: 10.1021/acs.iecr.3c03868.

[3] Badan Pusat Statistik, "Luas Panen dan Produksi Jagung di Indonesia 2024 (Angka Sementara)," 2024. [Online]. Available: https://www.bps.go.id/id/pressrelease/2024/10/15/2378/pada-2024--luas-panen-jagung-pipilan-diperkirakan-sebesar-2-58-juta-hektare-dan-produksi-jagung-pipilan-kering-dengan-kadar-air-14-persen-sebesar-15-21-juta-ton-.html

[4] B. Haryanto, I. T. Nasution, A. F. Polem, R. Tambun, and V. Alexander, "Natural Adsorbent of Corncob (Zea mays L.) Powder Capability in Purification of Used Cooking Oil with Shaking Operation Based on Turbidity," *Results Eng.*, vol. 19, Art. no. 101233, pp. 1–12, 2023, doi: 10.1016/j.rineng.2023.101233.

[5] M. A. Mardiah, Awitdrus, R. Farma, and E. Taer, "Characterization of Physical Properties for Activated Carbon from Garlic Skin," *J. Aceh Phys. Soc.*, vol. 10, no. 4, pp. 102–106, 2021, doi: 10.24815/jacps.v10i4.19571.

[6] R. Nandi, M. K. Jha, S. K. Guchhait, D. Sutradhar, and S. Yadav, "Impact of KOH Activation on Rice Husk Derived Porous Activated Carbon for Carbon Capture at Flue Gas alike Temperatures with High CO2 /N2 Selectivity," *ACS Omega*, vol. 8, no. 5,

pp. 4802–4812, 2023, doi: 10.1021/acsomega.2c06955.

[7] T. Attarbachi, M. Kingsley, and V. Spallina, "New Trends on Crude Glycerol Purification: A Review," *Fuel*, vol. 340, Art. no. 127485, pp. 1–19, 2023, doi: 10.1016/j.fuel.2023.127485.

[8] U. N. Fairuza, E. B. Corisa, I. K. Kusumaningrum, Y. Utomo, and A. Aliyatulmuna, "Investigating the Kinetics of Dye Adsorption of Methyl Orange (MO) Applying an Activated Carbon Adsorbent from Corncob Activated with $ZnCl_2$," *AIP Conf. Proc.*, vol. 3166, no. 1, pp. 1–9, Apr. 2025, doi: 10.1063/5.0236957.

[9] N. R. M. Aras and M. F. Lestari, "Uji Performa Pengaruh Gliserin dalam Formulasi Sabun Cair Cuci Piring," *Maj. Farmasetika*, vol. 9, no. 5, pp. 429–442, 2024, doi: 10.24198/mfarmasetika.v9i5.56837.

[10] Y. T. Khok, C. H. Ooi, A. Matsumoto, and F. Yeoh, "Reactivation of Spent Activated Carbon for Glycerine Purification," *Adsorption*, vol. 26, no. 7, pp. 1015–1025, Oct. 2020, doi: 10.1007/s10450-020-00210-x.

[11] Z. Heidarinejad, M. Dehghani, M. Heidari, G. Javedan, I. Ali, and M. Sillanpää, "Methods for Preparation and Activation of Activated Carbon: A Review," *Environ. Chem. Lett.*, vol. 18, no. 2, pp. 393–415, 2020, doi: 10.1007/s10311-019-00955-0.

[12] A. Sudibandriyo and A. Rizki, "The Influence of Activated Carbon as Adsorbent in Adsorptive – Distillation of Ethanol–Water Mixture," *Int. J. Technol.*, vol. 15, no. 2, pp. 425–431, 2024, doi: 10.14716/ijtech.v15i2.6659.

[13] L. M. Yuningsih, D. Mulyadi, and A. J. Kurnia, "Pengaruh Aktivasi Arang Aktif dari Tongkol Jagung dan Tempurung Kelapa terhadap Luas Permukaan dan Daya Jerap Iodin," *J. Kim. Val.*, vol. 2, no. 1, pp. 30–34, May 2016, doi: 10.15408/jkv.v2i1.3091.

[14] R. S. D. Lestari, D. K. Sari, A. Rosmadiana, and B. Dwipermata, "Pembuatan dan Karakterisasi Karbon Aktif Tempurung Kelapa dengan Aktivator Asam Fosfat Serta Aplikasinya Pada Pemurnian Minyak Goreng Bekas," *Tek. J. Sains Dan Teknol.*, vol. 12, no. 2, pp. 419–430, Oct. 2016, doi: 10.36055/tjst.v12i2.6607.

[15] M. P. Divya *et al.*, "Preparation and Characterization of Activated Carbon from Commercially Important Bamboo Species in North Eastern India," *Adv. Bamboo Sci.*, vol. 11, Art. no. 100148, pp. 1–9, May 2025, doi: 10.1016/j.bamboo.2025.100148.

[16] R. Dungani, S. S. Munawar, T. Karliati, J. Malik, P. Aditiawati, and Sulistyono, "Study of Characterization of Activated Carbon from Coconut Shells on Various Particle Scales as Filler Agent in Composite Materials," *J. Korean Wood Sci. Technol.*, vol. 50, no. 4, pp. 256–271, 2022, doi: 10.5658/WOOD.2022.50.4.256.

[17] S. Alam *et al.*, "Preparation of Activated Carbon from the Wood of Paulownia tomentosa as an Efficient Adsorbent for the Removal of Acid Red 4 and Methylene Blue Present in Wastewater," *Water*, vol. 13, no. 11, pp. 1–15, 2021, doi: 10.3390/w13111453.

[18] P. J. Wibawa, M. Nur, M. Asy'ari, and H. Nur, "SEM, XRD and FTIR Analyses of Both Ultrasonic and Heat Generated Activated Carbon Black Microstructures," *Heliyon*, vol. 6, Art. no. e03546, pp. 1–11, 2020, doi: 10.1016/j.heliyon.2020.e03546.

[19] E. Misran, B. K. S. Sipahutar, E. Sundari, and V. Pramananda, "One-Step Process of Glycerol Purification by Adsorption using Passion Fruit Peel-Based Activated Carbon," *Case Stud. Chem. Environ. Eng.*, vol. 11, Art. no. 101216, pp. 1–10, 2025, doi: 10.1016/j.cscee.2025.101216.

[20] Taslim, Iriany, O. Bani, E. Audina, and R. Hidayat, "Preparation of Activated Carbon-Based Catalyst from Nipa Palm (Nypa fruticans) Shell Modified with KOH for Biodiesel Synthesis,"

IOP Conf. Ser. Earth Environ. Sci., vol. 912, no. 1, pp. 1–6, 2021, doi: 10.1088/1755-1315/912/1/012094.

[21] E. A. Odja, I. Raya, Maming, M. Zakir, A. Karim, and D. N. Basir, "Characterization and Electrochemical Properties Analysis of Reduced Graphene Oxide from Corncob Carbon as an Electrode Candidate: Synthesized using modified Hummers method," *Commun. Sci. Technol.*, vol. 9, no. 1, pp. 25–29, 2024, doi: 10.21924/cst.9.1.2024.1365.

[22] Y. M. Abed, F. Allawi, F. S. Ali, S. J. Alhamd, T. A. Ibrahim, and M. N. Abbas, "Implementing a Sustainability Approach by Converting Plastic Bottle Waste from A Mischievous Substance to A Beneficial Material by Means of Zero Residue Level Concept," *Karbala Int. J. Mod. Sci.*, vol. 11, no. 3, pp. 396–411, 2025, doi: 10.33640/2405-609X.3413.

[23] E. L. Hanry, N. F. M. Redzwan, N. F. A. K. Badeges, and N. Surugau, "Characterization of biofilms developed from alginate extracted from Padina sp. incorporated with calcium chloride (CaCl2)," *J. Phys. Conf. Ser.*, vol. 2314, Art. no. 012022, pp. 1–13, 2022, doi: 10.1088/1742-6596/2314/1/012022.

[24] F. Yang, M. A. Kamarudin, P. Zhang, G. Kapil, T. Ma, and S. Hayase, "Enhanced Crystallization by Methanol Additive in Antisolvent for Achieving High-Quality MAPbI3 Perovskite Films in Humid Atmosphere," *ChemSusChem*, vol. 11, no. 14, pp. 2348–2357, 2018, doi: 10.1002/cssc.201800625.

[25] H. Hernando *et al.*, "Impact of Glycerol on Oil Palm Trunk Starch Bioplastics Enhanced with Citric-Acid Epoxidized Palm Oil Oligomers," *Case Stud. Chem. Environ. Eng.*, vol. 10, Art. no. 100839, pp. 1–14, 2024, doi: 10.1016/j.cscee.2024.100839.

[26] A. Ruzibayev, A. Abdurakhimov, O. Calvo-Gomez, S. Akhmedova, and S. Kurambayev, "Purification of Crude Glycerol Derived from Hydrogenated Cottonseed," *RURAL Sustain. Res.*, vol. 51, pp. 81–93, 2024, doi: 10.2478/plua-2024-0008.

[27] X. Liu, Q. Yu, A. Song, Dong S., and J. Hao, "Progress in Nuclear Magnetic Resonance Studies of Surfactant Systems," *Curr. Opin. Colloid Interface Sci.*, vol. 45, pp. 14–27, 2020, doi: 10.1016/j.cocis.2019.10.006.